Available online at www.sciencedirect.com
ScienceDirect
Journal of Molecular Graphics and Modelling 26 (2007) 93–103
Journal of Molecular Graphics and Modelling
www.elsevier.com/locate/JMGM

Optimization of electrostatics as a strategy for cold-adaptation: A case study of cold- and warm-active elastases

Elena Papaleo [a,b], Magne Olufsen [a], Luca De Gioia [b], Bjørn O. Brandsdal [a,*]

[a] The Norwegian Structural Biology Centre, Department of Chemistry, University of Tromsø, N9037 Tromsø, Norway
[b] Department of Biotechnology and Bioscience, University of Milano-Bicocca, P.za della Scienza 2, 20126 Milan, Italy

Received 13 June 2006; received in revised form 26 September 2006; accepted 26 September 2006
Available online 30 September 2006

Abstract

Adaptation to both high and low temperatures requires proteins with special properties. While organisms living at or close to the boiling point of water need to have proteins with increased stability, other properties are required at temperatures close to the freezing point of water. Indeed, it has been shown that enzymes adapted to cold environments are less resistant to heat with a concomitant increased activity as compared to their warm-active counter-parts. Several recent studies have pointed in the direction that electrostatic interactions play a central role in temperature adaptation, and in this study we investigate the role such interactions have in adaptation of elastase from Atlantic salmon and pig. Molecular dynamics (MD) simulations have been used to generate structural ensembles at 283 and 310 K of the psychrophilic and mesophilic elastase, and a total of eight 12 ns simulations have been carried out. Even though the two homologues have a highly similar three-dimensional structure, the location and number of charged amino acids are very different. Based on the simulated structures we find that very few salt-bridges are stable throughout the simulations, and provide little stabilization/destabilization of the proteins as judged by continuum electrostatic calculations. However, the mesophilic elastase is characterized by a greater number of salt-bridges as well as a putative salt-bridge network close to the catalytic site, indicating a higher rigidity of the components involved in the catalytic cycle. In addition, subtle differences are also found in the electrostatic potentials in the vicinity of the catalytic residues, which may explain the increased catalytic efficiency of the cold-adapted elastase.

Keywords: Molecular dynamics; Serine proteases; Cold adaptation; Psychrophilic enzyme; Electrostatics; Salt-bridge; Protein stability

1. Introduction

In permanently cold habitats, low temperatures have constrained psychrophilic or cold-adapted organisms to develop enzymatic tools allowing metabolic rates compatible to life and comparable to those of temperate organisms at their respective optimum temperatures [1,2]. Enzymes isolated from cold-adapted organisms are generally characterized by higher catalytic efficiency (k_{cat}/K_m) at low temperature in order to cope with the reduction of metabolic fluxes and chemical reaction rates [1,3]. A general theory for cold-adaptation has not yet been formulated since different enzymatic families can follow different evolutionary strategies [4,5]. Therefore, recently, the research community has focused on comparative structural investigations of homologous proteins adapted to different temperature conditions [6–8]. It turns out, however, that a high intrinsic structural flexibility of cold-adapted enzymes is generally accepted as the main adaptive strategy at low temperatures. An increased structural flexibility can reduce the activation energy necessary to generate reaction intermediates, resulting in a more efficient substrate turnover [1]. Increased intramolecular flexibility is achieved through weakening of interactions that stabilize the native protein molecules with a concomitant reduction in stability of cold-adapted enzymes [1,9].

Moreover, it is well accepted that among the various factors suggested to account for the greater stability of thermophilic proteins, the most consistent is the better optimized protein electrostatics [10,11]. On the contrary, the possible contribution of electrostatics towards active-site flexibility and proper solvation of psychrophilic proteins at low temperatures has only recently been considered [12]: in citrate synthase both the psychrophilic and the hyperthermophilic enzyme contain higher proportions of charged residues and salt-bridges than

* Corresponding author. Tel.: +47 77 64 40 57; fax: +47 77 64 47 65.
E-mail address: bjoerno@chem.uit.no (B.O. Brandsdal).

1093-3263/$ – see front matter
doi:10.1016/j.jmgm.2006.09.012

the mesophilic counterpart. The overall increased occurrence of charged residues in the psychrophilic enzyme ensures proper solvation at low temperature. The salt-bridges and their networks are also weaker and more dispersed in the psychrophilic enzyme, and the charged active-site residues are electrostatically more destabilizing, which possibly leads to a greater conformational flexibility. However, in other enzyme families, the psychrophilic enzyme even contains a lower number of salt-bridges than the mesophilic and thermophilic counterparts [5,13], but the salt-bridge contribution to protein stability has not yet been evaluated.

Intuitively, as stated above, one should expect that salt-bridges have stabilizing effects on the folded, native conformations of proteins. However, theoretical as well as experimental evaluation of the electrostatic strength of salt-bridges show that it varies significantly [11,14,15]. The contribution of salt-bridges to the free energy of folding of proteins ranges from being favourable in some cases to destabilizing in others, and in some proteins the contribution is virtually negligible. An early calculation by Honig and Hubbell estimated that the cost of transferring a salt-bridge from water to the protein environment is approximately 10–16 kcal/mol [16]. This large desolvation penalty, due to the burial of polar and charged groups in the protein interior during folding, is generally not recovered by favourable interactions in the folded state. Hence, an apparent paradox arises: on the one hand salt-bridges have been shown to frequently destabilize proteins [11,14,15], while on the other, salt-bridges are observed to be more frequent in thermophilic proteins than in their mesophilic and psychrophilic counter-parts [17].

In general, the hydration free energy of amino acids changes with temperature, which is caused by a decrease in the dielectric constant of water and the change in the contribution from entropic effects with the increase in temperature. The effects of temperature on protein hydration and the estimates of the free energies of folding of proteins, indicate a reduced desolvation penalty for salt-bridges at high temperatures [18]. This may explain the observed increase in the number of salt-bridges in the hyperthermophiles. Xiao and Honig have computed the electrostatic contributions to protein stability for four hyperthermophilic proteins and their mesophilic homologues [19]. They found that hyperthermophilic proteins have greater contributions from electrostatic interactions than their mesophilic homologues. Kumar et al. [18] observed that salt-bridges and their networks make a stabilizing contribution to the thermophilic glutamate dehydrogenase momomer, whereas, they contribute only marginally to the stability of the mesophilic glutamate dehydrogenase monomer. In the thermophilic enzyme, the desolvation penalty is offset largely by the cooperative, stabilizing effect of additional salt-bridges, often in the form of networks [18]. Electrostatic interactions also appear to become more favourable compared to hydrophobic interactions at higher temperatures [20], which may explain the increased occurrence of charged residues in thermophilic proteins [21].

Moreover, proteins exist in a range of conformations around their native states and the small variations among the different conformations involve changes in both hydrophobic and electrostatic interactions. In fact, the location of the charged residues and the geometry of their interactions are important factors in determining the electrostatic stabilities of salt-bridges and ion-pairs [10,11]. Observations on ion-pair movements and locations of charged residues in proteins suggest that salt-bridges in proteins may break and reform, pointing to a rather small energy difference between the two states [15]. Recently, a systematic study on a large number of salt-bridges in high-resolution protein crystal structures and NMR conformers has shown that the contributions of salt-bridges/ion-pairs to protein stability depend on the geometry of the charged pairing groups, and their environment in the structure [22]. The stabilities of almost all ion-pairs fluctuate, interconverting between stabilizing or destabilizing. If the interaction between the ion-pairing residues is stabilizing in the conformers that have high lifetimes, that ion-pair will be stabilizing to the protein structure. Salt-bridges observed in protein crystal structures may often break and reform in solution as a result of the movement of the charged residues. Other pairs of charged residues may come together and form salt-bridges either to compensate for the loss of salt-bridges observed in the crystal structure or in addition to the pre-existing salt-bridges.

The molecular basis of cold-adaptation of Atlantic salmon elastase (SE) has in this study been explored by means of MD simulations and continuum electrostatics calculations, and compared to its warm-active counter-part porcine elastase (PE). Given the strong dependency of the stabilizing/destabilizing contribution on geometry, structural and the exposed/buried environment, we investigate the electrostatic contributions of ion-pairs toward protein stability in ensembles of conformers around their native state. These ensembles also allow one to evaluate the sensitivity of electrostatic strength of charge–charge interactions to the variations in the orientation of the side-chains with respect to one another as well as their location in the protein. To carry out such an investigation, a range of conformers, which provide an adequate sampling of the conformational space around the native state, is required. It turns out that electrostatic interactions play a central role in temperature adaptation of elastase, influencing not only the protein stability but also probably modulating the catalytic efficiency.

2. Methods

2.1. Molecular dynamics simulations

MD simulations were performed using the Gromacs software [23], implemented on a parallel architecture. The X-ray structures of native porcine (PE) and Atlantic salmon elastase (SE) (PDB entries 1LVY [24] and 1ELT [25], respectively) were used as starting points for the MD simulations. Protein structures, including the crystallographic water molecules and calcium ions, were placed in a dodecahedral box of SPC water molecules [26]. The minimum distance between solute atoms and the box edge was set to 5 Å. The ionization state of charged residues was set to be consistent with neutral pH: Lys and Arg residues were positively charged,

whereas, Asp and Glu were negatively charged. The tautomeric form of histidine residues was derived using Gromacs tools and confirmed by visual inspection of the molecular environment of each histidine. Initially, solvent molecules were relaxed by molecular mechanics (steepest descent method, 100 steps). The minimization was followed by 20 ps MD at 300 K (time step 1 fs) while restraining protein atomic positions using a harmonic potential. During equilibration, the coupling constant of the external bath [27] was set to 0.001 ps for both protein and non-protein elements. MD simulations were performed in the NPT ensemble at 283 and 310 K, applying periodic boundary conditions and using an external bath with a coupling constant of 0.1 ps [27]. Pressure was kept constant (1 bar) by modifying the box dimensions and the time-constant for the pressure coupling was set to 1 ps [27]. The LINCS algorithm [28] was used to constrain bond lengths of heavy atoms, allowing the use of a 2 fs time step. Van der Waals and Coulomb interactions were truncated at 10 Å, while long-range electrostatic interactions were evaluated using the particle-mesh Ewald summation scheme [29]. The production phase consisted of 12 ns trajectories and collecting conformations every 2 ps. To improve the conformational sampling, two simulations at the same temperature, obtained using different initial velocities, were carried out for each of the elastases. Based on the rmsd as a function of time the stable part of the simulations was defined as the last 7.5 ns. Conformations from the stable part of the two simulations were then merged and subsequently analyzed. Investigation of these structures shows that the coordination of the calcium ions, which is important for both function and stability of elastases [30], is maintained throughout the simulations (results not shown). The visual analysis of the three-dimensional structures was carried out using VMD [31] and PyMOL (http://www.pymol.org), with particular regard to the localization of the charged residues in the structures.

2.2. Analysis of solvent accessibility degree and salt-bridges

The solvent accessibility degree of charged amino acids was computed using the NACCESS program [32] on conformations stored every 40 or 400 ps from the trajectories. The solvent accessibility profile of each charged residue and the corresponding average value are used to discriminate among buried and surface exposed charged residues. To discriminate between free charged residues and residues involved in salt-bridge formation the following strategy was pursued. Residues in the range of 4 Å from the side-chain oxygen atoms of aspartate and glutamate residues were monitored during the MD simulations. In particular, the persistency degree of each residue was defined as the ratio between the number of times that a residue appears in the surrounding of a determined oxygen atom and the total number of the conformations analyzed. Only the positively charged residues (arginine and lysine) present in the surrounding of each oxygen atom were selected and further analyzed. In particular, the attention was focused on Arg/Lys residues showing a persistency degree >10% in the surrounding of a determined oxygen atom. The distance between side-chain oxygen atom of Asp or Glu residues and side-chain nitrogen atom of positively charged residues (characterized by P-degree > 10%) was analyzed in details with regard to their evolution during the simulation.

2.3. Electrostatic calculations

In the second part of the work continuum electrostatics calculations using the Delphi program [33] were carried out on snapshots form the simulations collected every 400 ps and on the average structures obtained by the cluster analysis. The calculations were performed using the PARSE3 set [34] of atomic radii and the partial charges according to the Gromos force field [35]. The PARSE set allows reproduction of the experimental data for a wide range of small organic molecules and ions representing side-chains of amino acids [36]. The solvent probe radius used to define the molecular surface was 1.4 Å. The Poisson equation was solved using the iterative finite difference method. In each calculation, the molecule occupied 50% of the grid and Debye–Huckel (full Coulombic) boundary conditions were applied. The resulting grid of this calculation was adopted as boundary condition for two further focused calculations in which the molecule occupied 95% of the grid. Only the results of the focused calculation are presented here. All electrostatic calculations assumed pH 7 and zero ionic strength and the temperature of the simulation, since current implementation of Delphi correctly computes the reaction field energies only at zero ionic strength. The reaction field energy gives an accurate estimate of the electrostatic solvation energy (Delphi manual). Extensive testing reported in the literature [15] indicates that ionic strength does not affect appreciably the final values. The calculations were performed using a water dielectric constant of 80, while the protein dielectric constant (ε_p) attained different values: 4, 8, 10 and 20.

The electrostatic contribution of salt-bridges toward protein stability has been computed with respect to the corresponding hydrophobic isosteres. The hydrophobic isosteres correspond to the charged residues with all partial atomic charges set to zero [15,37]. This method has frequently been used in the literature [10,12,15,18,19,37]. The total electrostatic free energy contribution $\Delta\Delta G_{tot}$ of an ion-pair can be considered to correspond to the sum of three free energy terms [15]: the desolvation energy penalty, $\Delta\Delta G_{dslv}$, the bridge energy term $\Delta\Delta G_{brd}$, and the protein energy term $\Delta\Delta G_{prt}$ ($\Delta\Delta G$ is Gibbs free energy). $\Delta\Delta G_{dslv}$ is the energy penalty incurred by ion-pairing residues due to the desolvation of the charged side-chains in the folded state of the protein with respect to the unfolded state. $\Delta\Delta G_{brd}$ represents the electrostatic interaction between the charged groups in ion-pairing residue side-chains. $\Delta\Delta G_{prt}$ reflects the electrostatic interactions between the charged groups of the ion-pair and those in the remainder of the protein. Delphi outputs the energy values in units of kT, where k is Boltzmann constant and T is the temperature. The conversion factor between kT and kcal/mol is temperature dependent and we have used 283 and 310 K when converting.

```
SE          VVGGRVAQPNSWPWQISLQYKSGSSYYHTCGGSLIRQGWVMTAAHCVDSARTWRVVLGEH   60
PE          VVGGTEAQRNSWPSQISLQYRSGSSWAHTCGGTLIRQNWVMTAAHCVDRELTFRVVVGEH   60
            ****  ** **** ******:****: *****:****.**********   *:***:***

SE          NLNTNEGKEQIMTVNSVFIHSGWNSDDVAGGYDIALLRLNTQASLNSAVQLAALPPSNQI   120
PE          NLNQNNGTEQYVGVQKIVVHPYWNTDDVAAGYDIALLRLAQSVTLNSYVQLGVLPRAGTI   120
            *** *:*.** : *:.:.:*. **:****.*********  ..:*** ***..** :. *

SE          LPNNNPCYITGWGKTSTGGPLSDSLKQAWLPSVDHATCSSSGWWGSTVKTTMVCAGG-GA   179
PE          LANNSPCYITGWGLTRTNGQLAQTLQQAYLPTVDYAICSSSSYWGSTVKNSMVCAGGDGV   180
            *.**.******** * *.* *:::*:**:**:**:* ****.:******.:****** *.

SE          NSGCNGDSGGPLNCQVNGSYYVHGVTSFVSSSGCNASKKPTVFTRVSAYISWMNGIM---   236
PE          RSGCQGDSGGPLHCLVNGQYAVHGVTSFVSRLGCNVTRKPTVFTRVSAYISWINNVIASN   240
            .***:*******:* ***.* *********  ***.::***************:*.::
```

Fig. 1. Pair-wise sequence alignment of SE and PE. The identical (asterisk) and similar residues (double points) are highlighted. The charged residues are highlighted in grey.

3. Results and discussions

3.1. 3D localization and solvent accessibility degree of the charged residues

The 3D structure of elastases is folded into two juxtaposed domains characterized by an antiparallel β type fold: 12 β-strands and 3 α-helices are present in both SE and PE. The difference in the distribution of charged residues between SE and PE is mainly located in the C-terminal domain. This is particularly ascribable to the content in arginine residues, which is about six-fold higher in the C-terminal domain of PE than of SE (Fig. 1 and Table 1), which is in agreement with a low relative arginine content [Arg/(Arg + Lys)], a typical characteristic of several cold-adapted enzymes [2,4,5,7]. It has been suggested that lysine residues stabilize the folded state through increased rotameric states and thereby reducing the entropic penalty of going from the unfolded to the folded state when compared to arginine [38]. SE has 7 Lys and 6 Arg residues while the corresponding numbers are 3 and 12 for PE, and from an entropic point of view this will increase the stability of the SE relative to PE. On the contrary, arginine has a higher hydrogen bonding potential than lysine, and the greater number of arginine residues in PE thus adds more stability to PE. Moreover, from the pair-wise sequence alignment, it turns out that not only is the number of charged residues different in the psychrophilic and the mesophilic enzyme but also that only 16 charged residues are aligned with identical residues in the two proteins (Fig. 1). Therefore, the charged residues in the two proteins have been further analyzed with particular attention to

Table 1
Distribution of charged amino acids in SE and PE

	SE	PE
Total number of charged residues	23	26
Glutamate	3 (3 N-term)	4 (4 N-term)
Aspartate	7 (4 N-term/3 C-term)	7 (4 N-term/3 C-term)
Lysine	7 (2 N-term/5 C-term)	3 (1 N-term/2 C-term)
Arginine	6 (5 N-term/1 C-term)	12 (6 N-term/6 C-term)

The total number of each charged residues is indicated as well as the number of charged residues in the N-terminal (N-term) and C-terminal (C-term) domains.

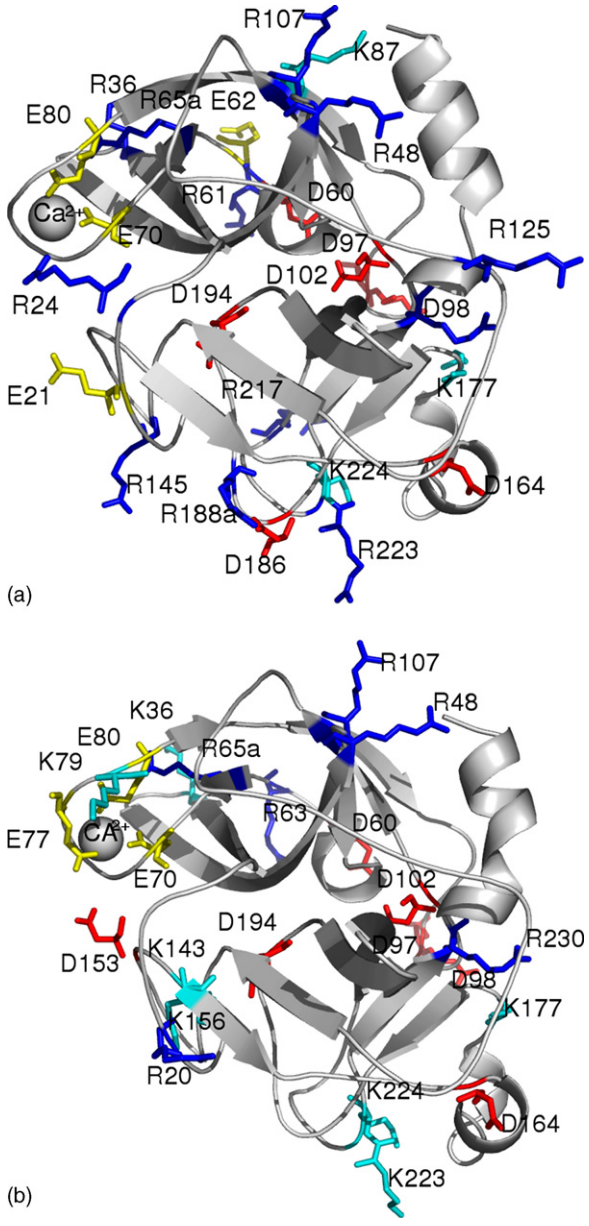

Fig. 2. Localization of the charged residues in the 3D-structure. The calcium ion and the secondary structure elements are indicated as light grey sphere and ribbon, respectively. The glutamate, aspartate, arginine and lysine residues in PE (A) and SE (B) are indicated as yellow, red, blue and cyan sticks, respectively.

their localization in the 3D-structures (Fig. 2). Indeed, a very different distribution of charged residues is observed when comparing the structures of the mesophilic and the psychrophilic elastase. In particular the distribution of the positively charged residues is very different in the two proteins with few residues occupying equivalent structural positions. Interestingly, the dielectric response of the protein has been suggest to correlate with thermostability [39], indicating that the arrangement of charged residues and their dynamics can be important in temperature adaptation.

The solvent accessibility of the charged residues is an important parameter to consider when calculating the electrostatic contribution toward protein stability [10,11,18], and this parameter was therefore evaluated during the MD trajectories (Table 2). The threshold to discriminate among buried and accessible amino acid side-chains was set to 30%. Amino acids with a solvent accessibility degree close to the fixed threshold were further analyzed by visual inspection to fully discriminate between solvent exposed and buried side-chains. Some values are above 100% which is ascribable to the procedure adopted by the program NACCESS in order to calculate the relative solvent accessibility degree. The reference for the calculation which should represent the ''condition of maximum solvent accessibility'' is a tripeptide structure A-x-A, where the residue x is surrounded by alanine residues [32]. Side-chains with a solvent exposure greater than 100% are located in surface regions where the side-chain is more solvent-exposed than in the tripeptide adopted as a reference by NACESS.

Most of the charged residues are solvent or partially solvent exposed with the exception of the glutamate residues that are involved in the coordination of the calcium ion and Asp102 and Asp194, and Arg230 in SE. Several charged residues show relevant fluctuations with respect to the average value of solvent accessibility during the simulations (Table 2). The highly solvent exposed charged residues are generally characterized by greater fluctuations in comparison to those, which are partially or totally buried in the protein core. This indicates that there are only few and not stable interactions with their surrounding, as one could expect from charged residues at the surface.

Table 2
Average solvent accessibility degree (%) of charged side-chains during the MD trajectories

	PE 283 K	PE 310 K	SE 283 K	SE 310 K
60 ASP	*54.26% (15.51)*	*69.75% (25.19)*	*70.41% (16.27)*	*78.52% (17.19)*
97 ASP	*105.92% (5.28)*	*103.47% (8.12)*	*104.21% (6.32)*	*101.22% (9.19)*
98 ASP	*62.90% (11.12)*	*57.51% (12.29)*	*51.78% (20.05)*	*49.71% (13.68)*
102 ASP	6.29% (4.55)	6.47% (4.49)	3.29% (5.60)	4.28% (4.01)
153 ASP	–	–	*68.61% (9.21)*	*67.41% (9.01)*
164 ASP	*48.70% (11.68)*	*48.91% (15.03)*	*55.57% (20.39)*	*70.23% (11.43)*
186 ASP	*42.38% (11.56)*	*43.57% (10.72)*	–	–
194 ASP	2.36% (1.55)	4.77% (2.73)	3.39% (2.82)	1.64% (1.30)
21 GLU	*63.71% (7.41)*	*64.00% (7.09)*	–	–
62 GLU	*85.00% (17.26)*	*78.74% (19.09)*	–	–
70 GLU	3.87% (3.32)	4.17% (2.55)	6.95% (2.75)	4.52% (1.71)
77 GLU	–	–	16.17% (4.55)	9.75% (4.52)
80 GLU	10.11% (5.22)	6.20% (4.22)	17.40% (6.06)	17.58% (4.06)
20 ARG	–	–	*63.93% (13.60)*	*69.26% (12.93)*
24 ARG	*75.03% (18.41)*	*52.23% (15.15)*	–	–
36 ARG	*51.92% (6.70)*	*48.54% (8.06)*	–	–
48 ARG	*47.00% (7.90)*	*44.24% (8.07)*	*49.80% (6.82)*	*49.19% (7.15)*
61 ARG	*72.44% (17.84)*	*58.70% (26.43)*	–	–
63 ARG	–	–	*47.90% (8.13)*	*62.43% (18.25)*
65A ARG	*31.76% (8.33)*	*33.39% (7.63)*	*24.76% (4.18)*	*34.08% (7.29)*
107 ARG	*30.05% (7.04)*	*24.79% (7.61)*	*40.69% (9.73)*	*38.08% (6.55)*
125 ARG	*91.43% (9.17)*	*79.50% (17.30)*	–	–
145 ARG	*67.79% (8.88)*	*73.02% (8.65)*	–	–
188A ARG	*42.12% (6.25)*	*42.00% (7.00)*	–	–
217A ARG	*83.88% (16.81)*	*59.88% (15.19)*	–	–
223 ARG	*67.30% (8.35)*	*64.40% (12.61)*	–	–
230 ARG	*25.37% (7.00)*	*27.00% (7.36)*	11.92% (4.77)	17.55% (6.48)
36 LYS	–	–	*43.41% (4.39)*	*47.40% (7.89)*
79 LYS	–	–	*60.71% (15.43)*	*63.60% (12.14)*
87 LYS	*58.19% (9.55)*	*64.86% (14.89)*	–	–
143 LYS	–	–	*26.52% (5.44)*	*25.10% (5.19)*
156 LYS	–	–	*27.69% (7.01)*	*23.99% (8.42)*
177 LYS	*59.24% (7.55)*	*57.13% (8.39)*	*57.35% (9.99)*	*51.36% (19.96)*
223 LYS	–	–	*71.58% (12.16)*	*57.49% (10.51)*
224 LYS	*35.30% (8.17)*	*38.10% (7.72)*	*63.36% (18.98)*	*30.09% (14.96)*

Standard deviations are given in parentheses. The side-chains with a solvent accessibility degree greater than the fixed threshold are given in italics and (–) indicates that in the corresponding position charged residues are missing.

Table 3
Ion-pair formation in the MD trajectories and their persistency degree

	PE 283 K	PE 310 K	SE 283 K	SE 310 K
21E_OE1	24Arg (2.51%)			
21E_OE2	24Arg (1.95%)			
62E_OE1	**61Arg (20.61%)**	**61Arg (10.23%)**		
62E_OE2	**61Arg (16.16%)**	36Arg (0.77%)		
		61Arg (7.67%)		
80E_OE1	24Arg (0.84%)	24Arg (1.79%)		
80E_OE2	24Arg (0.28%)			
60D_OD1	**61Arg (43.18%)**	**61Arg (42.71%)**	**63Arg (42.32%)**	**63Arg (12.90%)**
60D_OD2	**61Arg (40.11%)**	**61Arg (42.97%)**	**63Arg (38.01%)**	**63Arg (17.74%)**
97D_OD1				**177Lys (10.22%)**
97D_OD2				**177Lys (11.02%)**
98D_OD1	**177Lys (8.08%)**	**177Lys (28.64%)**	**177Lys (26.15%)**	**177Lys (20.16%)**
		217aArg (0.26%)		
98D_OD2	**177Lys (10.31%)**	**177Lys (26.60%)**	**177Lys (27.22%)**	**177Lys (23.12%)**
		217aArg (0.26%)		
153D_OD1				156Lys (0.27%)
153D_OD2				156Lys (0.27%)
164D_OD1				223Lys (0.81%)
164D_OD2	230Arg (1.11%)			223Lys (0.54%)
186D_OD1	**188aArg (92.76%)**	**188aArg (76.21%)**		
186D_OD2	**188aArg (95.82%)**	**188aArg (75.96%)**		
	223Arg (1.95%)	**223Arg (18.67%)**		

Positively charged residues with a P-degree close to or greater than 10% are highlighted in bold.

3.2. Salt-bridges and free charged residues as time-functions

Residues within 4 Å from the side-chain oxygen atoms of aspartate and glutamate residues were monitored during the MD simulations and the persistency degree (P-degree) of positively charged residues (arginine and lysine) have been evaluated as described in Section 2. The distance between side-chain oxygen atoms of Asp or Glu residues and side-chain nitrogen atoms of positively charged residues (characterized by P-degree $> 10\%$) has been analyzed in details with regard to their evolution during the simulation (Table 3). Among the putative ion-pairs only a few of them present suitable distances to be classified as a salt-bridge in a sufficiently large part of the MD conformations. The ion-pairs E62-R61, D60-R61, D98-K177 and D186-R188a have been selected in PE simulations, whereas, the ion-pairs D60-R63 and D98-K177 have been selected in SE simulations.

The mesophilic elastase is characterized by a higher number of salt-bridges and also a putative salt-bridge network, in which the D60-R61-E62 triad seems to be involved. Most of the residues involved in the formation of salt-bridges in PE are not

Table 4
Ion-pair distances during the MD simulations

	PE 283 K (Å)	PE 310 K (Å)	SE 283 K (Å)	SE 310 K (Å)
D60-R61/R63				
Average	7.0 (1.8)	6.9 (1.9)	6.4 (1.5)	9.2 (3.6)
Min–Max	3.2–9.7	3.4–8.9	3.4–9.3	4.3–15.9
E62-R61				
Average	8.9 (2.7)	14.2 (3.8)		
Min–Max	4.3-12.7	8.3-21.0		
D98-K177				
Average	6.5 (1.5)	6.4 (2.1)	7.2 (2.5)	7.1 (2.0)
Min–Max	3.4–9.5	3.1–10.9	2.9–10.1	3.2–11.0
D186-R188a				
Average	4.5 (1.6)	5.5 (2.5)		
Min–Max	3.0–6.7	3.2–11.3		

For each pair, the average, minimum (Min) and maximum (Max) distances between the side-chain of the positive charged residue and the side-chain of the negative charged residue during the MD trajectories are reported in this table. The standard deviation is indicated in parenthesis.

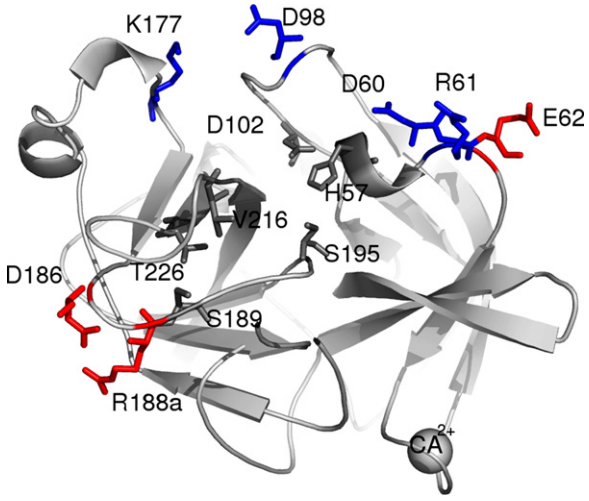

Fig. 3. Localization of the ion-pairs on the 3D-structure. The calcium ion and the secondary structure elements are indicated as light grey sphere and ribbon, respectively. The ion-pairing residues and residues of the catalytic site and the specificity pocket are indicated in blue (conserved ion-pairs in both SE and PE) or red (ion-pairs present only in PE) and black, respectively.

conserved in the psychrophilic enzyme, such as E62, D186 and R188a. Moreover, it is interesting to note that in the ion-pairs common between PE and SE, the persistency degree is generally greater in the PE simulations (Table 3), while all the residues involved in ion-pairs in the two proteins present a high degree of solvent accessibility. The only ion pair that has a higher P-degree in SE is the D98-K177 ion pair in the 283 K simulations, but when comparing the results from the habitat temperature similar P-degrees are observed (Table 3).

Extensive analysis of salt-bridges in a large dataset of structurally non-redundant high-resolution crystal structures of proteins demonstrated that salt-bridges could be destabilizing or stabilizing to the protein, depending on three factors [40]: (i) the buried/exposed location of the ion-pairing residues in the protein structure; (ii) the distance and geometric orientation of the side-chain charged groups with respect to each other; and (iii) the interaction of the charged groups in the salt-bridge with the charged groups in the remainder of the protein. In particular, the analysis indicated that most ion-pairs obeying the geometric definition of a salt-bridge stabilize the native state of proteins. In contrast, those with distances exceeding the 4.0 Å limits largely contribute to destabilize the folded protein structure. Thus, the distance between the two salt-bridging residues was monitored during the MD trajectories, and particular regard has been directed towards their average, minimum and maximum value (Table 4).

Table 4 shows that the MD ensembles represent a broad spectrum of ion-pair movements. During the trajectories the residues forming the ion-pairs frequently move out of or come back to be within salt bridging distances, which is in agreement

Table 5
Stabilities of the ion-pairs in SE and PE MD ensembles

	Conformation ensemble	$\Delta\Delta G_{dslv}$ (kcal/mol)	$\Delta\Delta G_{brd}$ (kcal/mol)	$\Delta\Delta G_{prt}$ (kcal/mol)	$\Delta\Delta G_{tot}$ (kcal/mol)
D60-R61	PE 283 K 35 conformations	Av: 1.142 (0.409) Min: 0.451 Max: 2.074	Av: −0.200 (0.147) Min: −0.731 Max: −0.055	Av: −0.189 (0.292) Min: −0.698 Max: 0.391	Av: 0.753 (0.169) Min: 0.090 Max: 0.807
D60-R61	PE 310 K 39 conformations	Av: 1.448 (0.439) Min: 0.529 Max: 2.216	Av: −0.662 (0.205) Min: −1.194 Max: −0.399	Av: −0.413 (0.399) Min: −1.414 Max: 0.277	Av: 0.373 (0.217) Min: −0.145 Max: 0.660
D60-R63	SE 283 K 36 conformations	Av: 1.377 (0.223) Min: 0.865 Max: 1.787	Av: −0.639 (0.126) Min: −0.930 Max: −0.366	Av: −0.510 (0.258) Min: −1.232 Max: −0.036	Av: 0.228 (0.130) Min: −0.112 Max: 0.402
D60-R63	SE 310 K 36 conformations	Av: 1.141 (0.420) Min: 0.311 Max: 1.971	Av: −0.534 (0.262) Min: −1.116 Max: −0.401	Av: −0.193 (0.291) Min: −0.923 Max: 0.393	Av: 0.415 (0.184) Min: −0.162 Max: 0.644
E62-R61	PE 283 K 35 conformations	Av: 0.783 (0.351) Min: 0.219 Max: 1.534	Av: −0.410 (0.165) Min: −0.733 Max: −0.227	Av: −0.718 (0.352) Min: −1.689 Max: −0.143	Av: −0.345 (0.191) Min: −0.672 Max: 0.285
E62-R61	PE 310 K 39 conformations	Av: 1.288 (0.756) Min: 0.221 Max: 2.759	Av: −0.447 (0.132) Min: −0.750 Max: −0.262	Av: −1.404 (0.688) Min: −2.577 Max: −0.057	Av: −0.563 (0.756) Min: −0.879 Max: 0.244
D98-K177	PE 283 K 35 conformations	Av: 1.326 (0.375) Min: 0.527 Max: 2.494	Av: −0.701 (0.223) Min: −1.534 Max: −0.417	Av: −0.441 (0.341) Min: −1.220 Max: 0.131	Av: 0.184 (0.139) Min: −0.266 Max: 0.380
D98-K177	PE 310 K 39 conformations	Av: 1.809 (0.551) Min: 0.945 Max: 2.808	Av: −0.954 (0.433) Min: −1.821 Max: −0.351	Av: −0.653 (0.351) Min: −1.430 Max: −0.039	Av: 0.202 (0.558) Min: −0.168 Max: 0.558
D98-K177	SE 283 K 36 conformations	Av: 1.737 (0.615) Min: 0.888 Max: 3.039	Av: −0.787 (0.500) Min: −1.752 Max: −0.337	Av: −0.783 (0.294) Min: −1.455 Max: 0.108	Av: 0.205 (0.174) Min: −0.135 Max: 0.624
D98-K177	SE 310 K 36 conformations	Av: 1.868 (0.597) Min: 0.965 Max: 3.161	Av: −0.769 (0.391) Min: −2.250 Max: −0.374	Av: −0.931 (0.450) Min: −1.922 Max: −0.208	Av: 0.168 (0.158) Min: −0.179 Max: 0.539
D186-R188a	PE 283 K 35 conformations	Av: 2.379(0.648) Min: 1.055 Max: 3.867	Av: −1.171 (0.386) Min: −1.827 Max: −0.276	Av: −1.155 (0.325) Min: −1.714 Max: −0.516	Av: 0.054 (0.163) Min: −0.282 Max: 0.385
D186-R188a	PE 310 K 39 conformations	Av: 2.434(0.688) Min: 1.561 Max: 4.171	Av: −1.068 (0.483) Min: −1.999 Max: −0.336	Av: −1.328 (0.282) Min: −1.799 Max: −0.545	Av: 0.038 (0.220) Min: −0.435 Max: 0.523

Min, Max and Av denote the minimum, maximum and average values of the $\Delta\Delta G$ terms in the MD ensembles, respectively. The standard deviations for the average values are indicated in parenthesis. For clarity only the results relative to the calculation with $\varepsilon_p = 20$ are indicated.

with previous findings [22]. While some ion-pairs tend to remain at almost constant distances, others show extensive movements (Table 4). In fact, in some cases the distance between the two charged residues have standard deviations as large as 2.5–3.8 Å around their average values (Table 4). Only D186-R188a and D98-K177 survive as salt-bridges in a large number of the conformations in each ensemble, whereas, the other ion-pairs are defined as salt-bridges only in a minority of the conformations (Table 4). Moreover, if we consider the distance between the salt-bridging residues as a geometry parameter, the salt-bridges of the mesophilic elastase are better optimized. The additional salt-bridges found in PE (E62-R61 and D186-R188a) are localized in the vicinity of the catalytic histidine (H57) and close to the substrate specificity pocket (Fig. 3).

Additional evidence for the movement of the charged residues can be derived from their solvent accessible surfaces, as previously described (Table 2). A small accessible surface area (ASA) for a residue indicates that it is mostly buried, whereas, a large value implies that it is at or close to the molecular surface. The location of the charged residues in the protein structure is not fixed during the simulations, and significant fluctuations are observed (Table 2). Taken together, these data give a dynamic scenario of salt-bridges in proteins, where charged residues can move apart and then get closer in different conformations of the ensembles, in agreement with previous findings on a database of protein ensembles obtained by NMR spectroscopy [22].

3.3. Continuum electrostatics calculations of salt-bridges

The electrostatic contribution to the free energy from each ion-pair has been calculated in all the selected conformations from the MD trajectories (see Section 2). Each calculation yields the following energy terms: the total electrostatic contribution to the free energy of the ion-pair formation $\Delta\Delta G_{tot}$, the desolvation energy ($\Delta\Delta G_{dslv}$) for the charged residues in the folded state of the protein, the bridging energy term ($\Delta\Delta G_{brid}$) for the electrostatic interaction between the charges forming the ion-pairing, and the protein energy term ($\Delta\Delta G_{prt}$) for the electrostatic interaction between the ion-pair and the rest of the

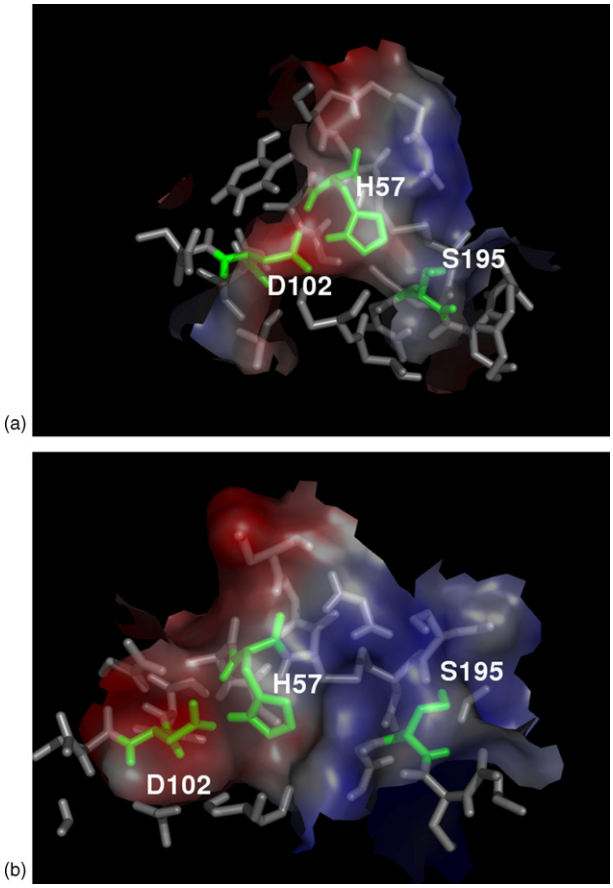

Fig. 4. Electrostatic potential surface in the proximity of the active site in PE. The electrostatic potential surface of the average structure of PE at 283 K (A) and 310 K (B) is indicated: red, blue and white regions indicated negative, positive and apolar regions on the surface, respectively. The catalytic triad (H57, D102 and S195) are highlighted as green sticks, whereas, the amino acids within 5 Å of the catalytic triad are indicated as grey sticks. For clarity, the average structure relative to the first cluster of the MD simulations is reported.

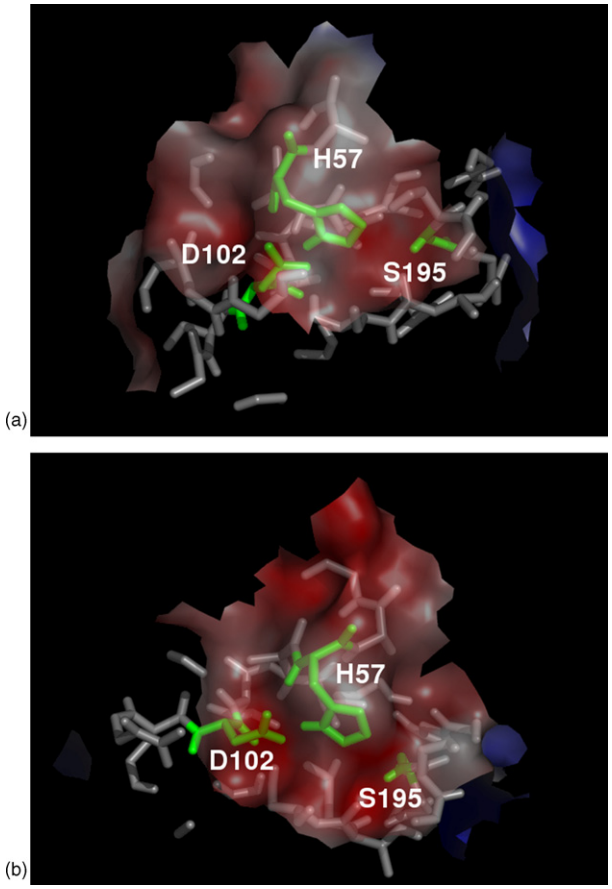

Fig. 5. Electrostatic potential surface in the proximity of the active site in SE. The electrostatic potential surface of the average structure of SE at 283 K (A) and 310 K (B) is indicated: red, blue and white regions indicated negative, positive and apolar regions on the surface, respectively. The catalytic triad (H57, D102 and S195) are highlighted as green sticks, whereas, the amino acids within 5 Å of the catalytic triad are indicated as grey sticks. For clarity, the average structure relative to the first cluster of the MD simulations is reported.

protein. These energy terms are related to each other by the following equation:

$$\Delta\Delta G_{tot} = \Delta\Delta G_{dslv} + \Delta\Delta G_{brd} + \Delta\Delta G_{prt}$$

When considering the average, minimum, and maximum values of these terms for each ion-pair in the structural ensembles (Table 5), it turns out that the strength of the ion-pairs varies a lot between different conformations. We have also investigated the effect of different protein dielectric constants (ε_p) spanning from 4 to 20 (see Section 2) and in agreement with previous results [12,41], the best value for ε_p seems to be 20, as the ion-pairing residues of SE and PE are all highly solvent exposed. The other values investigated tend to overestimate the energetic penalty arising from desolvation of the residues.

The salt-bridges present in SE and PE are only marginally stabilizing or destabilizing, with the electrostatic contribution to the free energy amounting to less than 1 kcal/mol (Table 5). However, the salt-bridges E62-R61 and D186-R188a present only in PE and not conserved in the psychrophilic counterpart are stabilizing and partially stabilizing in many conformations of the ensembles, highlighting a contribution to the greater stability of the mesophilic protein. On the contrary, the salt-bridges D98-K177 and D60-R61/R63, conserved in both proteins are almost always destabilizing (Table 5). The D60-R61/R63 ion pair has a slightly shorter average distance in the simulation of SE at 283 K when compared to PE (Table 4). The average electrostatic contribution also shows that it is slightly more destabilizing the mesophilic enzyme at low temperature, but of similar effect if we compare the energetic contribution the habitat temperatures (Table 5). However, the contribution toward stability from the D60-R61/R63 ion-pair is virtually identical in the two enzymes, as reflected by the standard deviations given in Tables 4 and 5. The electrostatic contribution to the stability of the enzymes, found by adding the ion-pairs present in each simulations in Table 5, is 0.65 and 0.43 kcal/mol at 283 K and 0.05 and 0.58 kcal/mol at 310 K for PE and SE, respectively. Hence, the ion-pairs in PE become more favourable when the temperature is increased to its habitat temperature.

3.4. Electrostatic potential surface in the proximity of functional relevant regions

Continuum electrostatics calculations were carried out not only on snapshots from the simulations but also on the average structures obtained with the cluster analysis, and the

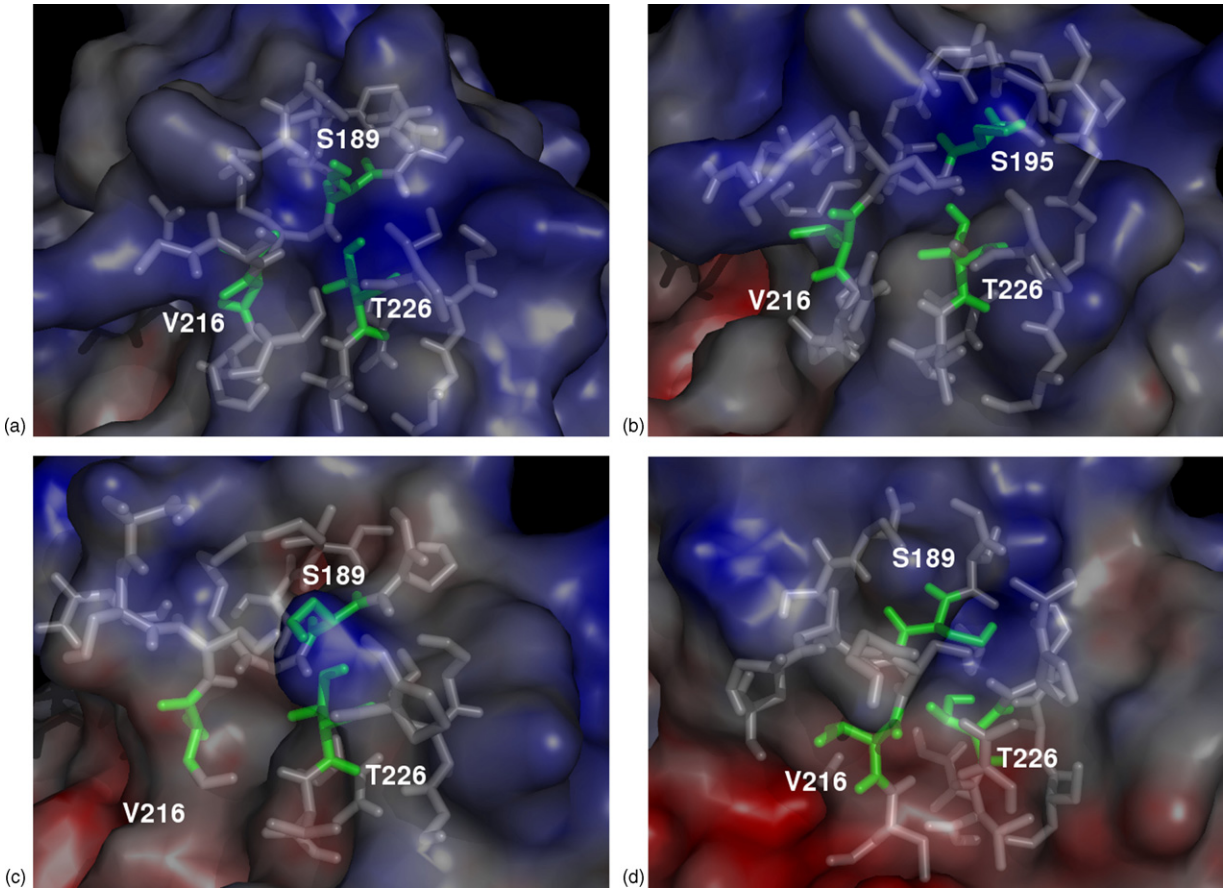

Fig. 6. Electrostatic potential surface in the proximity of the specificity pocket in PE and SE. The electrostatic potential surface of the average structure of PE (A, B) and SE (C, D) at 283 (A–C) and 310 K (B–D) is indicated: red, blue and white regions indicated negative, positive and apolar regions on the surface, respectively. The specificity pocket (S189, V216 and T226) are highlighted as green sticks, whereas, the amino acids within 5 Å of the specificity pocket residues are indicated as grey sticks. For clarity, the average structure relative to the first cluster of the MD simulations is reported. The average structures relative to the other cluster yielded to the same results (data not shown).

resulting electrostatic potential surfaces were further analyzed. First, the energies obtained from the Delphi calculations (i.e. grid energy, self-reaction field energy; correct reaction field energy, total reaction field energy and columbic energy) were analyzed with respect to their evolution during the time to ensure that the electrostatic surface was almost constant during the simulations. These profiles are stable during the trajectories indicating that the electrostatic surface is virtually constant throughout the simulations. Therefore, the electrostatic potential surface, calculated using the average structures, were considered as representative of the whole simulations and analyzed in details. The electrostatic potential surface of SE and PE at the same temperature are compared to highlight differences. In particular, the analysis focuses on the surroundings of the catalytic site residues (H57, D102, S195) and the specificity pocket residues (S189,V216, T226).

The electrostatic surface potentials around the active site are significantly different between the cold- and warm-adapted elastase at both temperatures. Fig. 4 shows that PE has a polarized electrostatic surface around the catalytic residues with negative potential localized between D102 and H57 and positive potential between the H57 and the nucleophile catalytic residue S195. SE has a surface characterized by negative potentials (Fig. 5) and a partially positive surface in the proximity of S195.

Thus, the electrostatic potential surface in the proximity of the specificity pocket shows that the mesophilic elastase is characterized by a positive potential around the specificity pocket (Fig. 6), which could assist the substrate recognition by electrostatic interactions. On the contrary, the psychrophilic elastase is characterized by a more hydrophobic surface, surrounded by some regions of positive potential in the proximity of the specificity pocket, which could account for an improved binding of the substrate in the pocket and which fits with the experimental evidence of a lower value of K_m for SE than for PE [42]. In fact, elastases are serine-proteases specific for aliphatic residues in P1 position [43].

4. Conclusions

The question of whether salt-bridges are stabilizing or destabilizing to protein structures has been frequently addressed in the experimental and computational literature. Our present investigation and previous observations on NMR conformer ensembles provide indications that there are fluctuations in the electrostatic interactions, illustrating that the electrostatic contribution of an ion-pair to protein stability is indeed conformation dependent [8,22]. If the interaction between the ion-pairing residues is stabilizing in the conformations that have high population times, that ion-pair will be stabilizing to the protein structure.

The psychrophilic elastase is characterized by a lower number of charged residues than the mesophilic counterpart, and in particular the psychrophilic elastase has fewer salt-bridges at the surface. On the basis of the previous observation, we can state that the salt-bridges present only in the mesophilic elastase are stabilizing or marginally stabilizing to the protein structure and their localization close to the active site or the specificity pocket accounts for their role in enzymes that could resist to high temperature, whereas, the psychrophilic elastase avoids the presence of a great number of salt-bridges across the active site in order to ensure structural flexibility. The present investigation has allowed us to pinpoint specific features that differentiate the cold-adapted elastase from its warm-adapted counterpart, and provides a scenario in which localized flexibility in strategically functional regions is the strategy pursued by the psychrophilic elastase and serine-proteases in general. In contrast, the mesophilic counterpart shows a scattered flexibility in none-functional regions and an additional stability in the surroundings of the active site and specificity pocket due to the presence of unique stabilizing ion-pairs.

Moreover, a detailed analysis of the electrostatic potential surface in the proximity of functionally relevant regions revealed interesting aspects of the psychrophilic elastase. In particular, the proximity of the specificity pocket, where the P1 position of the substrate is accommodated, a more hydrophobic surface, surrounded by positively charged regions is present in the psychrophilic elastase. Charged protein regions on the surface could improve the substrate recognition through optimized electrostatic interactions, whereas, the hydrophobic portion of the surface could account for a better binding of the substrate in the pocket, since elastase are serine-proteases specific for aliphatic side-chain at P1 position of the substrate. This observation is in agreement with experimental data [42], which shows that SE is characterized by a lower value of K_m than PE, indicating a greater affinity for the substrate. In addition, the catalytic nucleophile S195 is surrounded by a positively charged region, which may be functionally relevant to assist the nucleophile attack, activating the substrate and to provide additional stabilization of the negatively charged oxyanion intermediate. These observations are in good agreement with the hypothesis of a localized structural flexibility of the psychrophilic serine-proteases in crucial regions, surrounding the catalytic site.

Protein electrostatics is one of the major factors of thermostability and has been the focus of this study of cold- and warm-active elastases. It is, however, evident that nature can explore and use other factors in order to fine-tune the thermal stability of proteins. Folding of proteins involves reduction of the entropy of the polypeptide chain, and the conformational entropy will thus decrease when going from unfolded to folded proteins. The conformational entropy of the polypeptide chain will therefore favour the unfolded state.

Acknowledgements

The authors acknowledge financial support from the ''Progetto Nazionale Ricerche in Antartide'', Italy, and from the Research Council of Norway. The Norwegian Structural Biology Centre (NorStruct) is supported by the Functional Genomics Program (FUGE) of the Research Council of Norway.

References

[1] D. Georlette, V. Blaise, T. Collins, S. D'Amico, E. Gratia, A. Hoyoux, J.C. Marx, G. Sonan, G. Feller, C. Gerday, Some like it cold: biocatalysis at low temperatures, FEMS Microbiol. Rev. 28 (2004) 25–42.

[2] A.O. Smalås, H.K.S. Leiros, V. Os, N.P. Willassen, Biotechnology Annual Review, vol. 6, Elsevier Science B.V., Amsterdam, 2000.

[3] P.A. Fields, Review: Protein function at thermal extremes: balancing stability and flexibility, Comp. Biochem. Phys. A 129 (2001) 417–431.

[4] G. Gianese, P. Argos, S. Pascarella, Structural adaptation of enzymes to low temperatures, Protein Eng. 14 (2001) 141–148.

[5] G. Gianese, F. Bossa, S. Pascarella, Comparative structural analysis of psychrophilic and meso- and thermophilic enzymes, Proteins 47 (2002) 236–249.

[6] S. D'Amico, C. Gerday, G. Feller, Temperature adaptation of proteins: Engineering mesophilic-like activity and stability in a cold-adapted alpha-amylase, J. Mol. Biol. 332 (2003) 981–988.

[7] H.K.S. Leiros, N.P. Willassen, A.O. Smalås, Structural comparison of psychrophilic and mesophilic trypsins—elucidating the molecular basis of cold-adaptation, Eur. J. Biochem. 267 (2000) 1039–1049.

[8] A. Svingor, J. Kardos, I. Hajdu, A. Nemeth, P. Zavodszky, A better enzyme to cope with cold—comparative flexibility studies on psychrotrophic, mesophilic, and thermophilic IPMDHS, J. Biol. Chem. 276 (2001) 28121–28125.

[9] S. D'Amico, J.C. Marx, C. Gerday, G. Feller, Activity-stability relationships in extremophilic enzymes, J. Biol. Chem. 278 (2003) 7891–7896.

[10] S. Kumar, R. Nussinov, How do thermophilic proteins deal with heat? Cell Mol. Life Sci. 58 (2001) 1216–1233.

[11] S. Kumar, R. Nussinov, Close-range electrostatic interactions in proteins, Chembiochem 3 (2002) 604–617.

[12] S. Kumar, R. Nussinov, Different roles of electrostatics in heat and in cold: adaptation by citrate synthase, Chembiochem 5 (2004) 280–290.

[13] S. D'Amico, P. Claverie, T. Collins, D. Georlette, E. Gratia, A. Hoyoux, M.A. Meuwis, G. Feller, C. Gerday, Molecular basis of cold adaptation, Philos. T Roy Soc. B 357 (2002) 917–924.

[14] E. Bae, G.N. Phillips, Identifying and engineering ion pairs in adenylate kinases, J. Biol. Chem. 280 (2005) 30943–30948.

[15] Z.S. Hendsch, B. Tidor, Do salt bridges stabilize proteins—a continuum electrostatic analysis, Protein Sci. 3 (1994) 211–226.

[16] B.H. Honig, W.L. Hubbell, Stability of salt bridges in membrane-proteins, P. Natl. Acad. Sci.-Biol. 81 (1984) 5412–5416.

[17] A. Karshikoff, R. Ladenstein, Ion pairs and the thermotolerance of proteins from hyperthermophiles: a 'traffic rule' for hot roads, Trends Biochem. Sci. 26 (2001) 550–556.

[18] S. Kumar, B.Y. Ma, C.J. Tsai, R. Nussinov, Electrostatic strengths of salt bridges in thermophilic and mesophilic glutamate dehydrogenase monomers, Proteins 38 (2000) 368–383.

[19] L. Xiao, B. Honig, Electrostatic contributions to the stability of hyperthermophilic proteins, J. Mol. Biol. 289 (1999) 1435–1444.

[20] A.S. Thomas, A.H. Elcock, Molecular simulations suggest protein salt bridges are uniquely suited to life at high temperatures, J. Am. Chem. Soc. 126 (2004) 2208–2214.

[21] C. Cambillau, J.M. Claverie, Structural and genomic correlates of hyperthermostability, J. Biol. Chem. 275 (2000) 32383–32386.

[22] S. Kumar, R. Nussinov, Fluctuations in ion pairs and their stabilities in proteins, Proteins 43 (2001) 433–454.

[23] D. van der Spool, A.R. van Buuren, E. Apol, P.J. Meulenhoff, D.P. Tieleman, A.L.T.M. Sjibers, B. Hess, K.A. Feenstra, E. Lindahl, R. van Drunen, H.J.C. Berendsen, Gromacs User Manual version 3.1.1, Nijenborgh 4, 9747 AG Groningen, The Netherlands, www.gromacs.org, 2002.

[24] M. Schiltz, W. Shepard, R. Fourme, T. Prange, E. DeLaFortelle, G. Bricogne, High-pressure krypton gas and statistical heavy-atom refinement: a successful combination of tools for macromolecular structure determination, Acta Crystallogr. D 53 (1997) 78–92.

[25] G.I. Berglund, N.P. Willassen, A. Hordvik, A.O. Smalås, Structure of native pancreatic elastase from north-Atlantic Salmon at 1.61 angstrom resolution, Acta Crystallogr. D 51 (1995) 925–937.

[26] H.J.C. Berendsen, J.P.M. Postma, W.F.v. Gunsteren, J. Hermans, in: B. Pullman (Ed.), Intermolecular Forces, Riedel, 1981, pp. 331–342.

[27] H.J.C. Berendsen, J.P.M. Postma, W.F. Vangunsteren, A. Dinola, J.R. Haak, Molecular-dynamics with coupling to an external bath, J. Chem. Phys. 81 (1984) 3684–3690.

[28] B. Hess, H. Bekker, H.J.C. Berendsen, J.G.E.M. Fraaije, LINCS: a linear constraint solver for molecular simulations, J. Comput. Chem. 18 (1997) 1463–1472.

[29] T. Darden, D. York, L. Pedersen, Particle mesh Ewald—an NLog(N) method for Ewald sums in large systems, J. Chem. Phys. 98 (1993) 10089–10092.

[30] G. Jayaraman, S. Srimathi, J.B. Bjarnason, Conformation and stability of elastase from Atlantic cod, Gadus morhua, BBA 2006 (1760) 47–54.

[31] W. Humphrey, A. Dalke, K. Schulten, VMD: visual molecular dynamics, J. Mol. Graphics 14 (1996) 33–38.

[32] S. Hubbard, J. Thornton, Department of Biochemistry and Molecular Biology, University College London, London, 1993.

[33] K.A. Sharp, B. Honig, Electrostatic interactions in macromolecules—theory and applications, Annu. Rev. Biophys. Biol. 19 (1990) 301–332.

[34] D. Sitkoff, K.A. Sharp, B. Honig, Accurate calculation of hydration free-energies using macroscopic solvent models, J. Phys. Chem.-US 98 (1994) 1978–1988.

[35] L.D. Schuler, X. Daura, W.F. Van Gunsteren, An improved GROMOS96 force field for aliphatic hydrocarbons in the condensed phase, J. Comput. Chem. 22 (2001) 1205–1218.

[36] A. Radzicka, R. Wolfenden, Comparing the polarities of the amino-acids—side-chain distribution coefficients between the vapor-phase, cyclohexane, 1-octanol, and neutral aqueous-solution, Biochemistry-US 27 (1988) 1664–1670.

[37] S. Spector, M.H. Wang, S.A. Carp, J. Robblee, Z.S. Hendsch, R. Fairman, B. Tidor, D.P. Raleigh, Rational modification of protein stability by the mutation of charged surface residues, Biochemistry-US 39 (2000) 872–879.

[38] I.N. Berezovsky, W.W. Chen, P.J. Choi, E.I. Shakhnovich, Entropic stabilization of proteins and its proteomic consequences, PLOS Comput. Biol. 1 (2005) 322–332.

[39] B.N. Dominy, H. Minoux, C.L. Brooks, An electrostatic basis for the stability of thermophilic proteins, Proteins 57 (2004) 128–141.

[40] S. Kumar, R. Nussinov, Salt bridge stability in monomeric proteins, J. Mol. Biol. 293 (1999) 1241–1255.

[41] C.N. Schutz, A. Warshel, What axe the dielectric ''constants'' of proteins and how to validate electrostatic models? Proteins 44 (2001) 400–417.

[42] G.I. Berglund, A.O. Smalås, H. Outzen, N.P. Willassen, Purification and characterization of pancreatic elastase from North Atlantic salmon (Salmo salar), Mol. Mar. Biol. Biotech. 7 (1998) 105–114.

[43] L. Hedstrom, Serine protease mechanism and specificity, Chem. Rev. 102 (2002) 4501–4523.